

Article

Characterization of Thermal and Stress Dual-Induced Nano-SiC-Modified Microcapsules

Yunlong Sun ^{1,2}, Xiaoping Ji ² , Yueqin Hou ^{3,*} , Siqi Wang ^{2,*}, Ye Chen ^{2,4}, Lu Liu ² and Sijia Liu ¹

¹ Xinjiang Academy of Transportation Science, Co., Ltd., Urumqi 830000, China; sunyunlong6509@sina.com (Y.S.); liusijia64@gmail.com (S.L.)

² School of Highway, Chang'an University, Xi'an 710064, China; jixp82@163.com (X.J.); wchenye2@163.com (Y.C.); liulu_2002@163.com (L.L.)

³ School of Human Settlements and Civil Engineering, Xi'an Jiaotong University, Xi'an 710049, China

⁴ School of Transportation, Southeast University, Nanjing 211189, China

* Correspondence: houyueqin527@163.com (Y.H.); 2022021067@chd.edu.cn (S.W.); Tel.: +86-137-5997-2825 (Y.H.)

Abstract: This work reports a kind of thermal and stress dual-induced nano-SiC-modified microcapsule that is applied to asphalt pavement to improve its self-healing performance. For this purpose, the microcapsules needed to contain a regenerator and be stable in an asphalt mixture. In addition, the microcapsules needed to have good wave-absorbing and temperature-raising properties to realize the dual-mechanism-induced release of microcapsules. In the first step in this study, heat-stressed double microcapsules were prepared. Then, the properties of the microcapsules—including basic properties, stability, mechanical properties, and wave-absorbing and temperature-raising properties—were tested. Finally, the self-healing mechanism of the microcapsules was observed. The results show that the nano-SiC-modified microcapsules have a high core content (87.6%), suitable particle size (average particle size of 53.50 μm), high thermal stability (mass loss of 2.92% at 150–170 $^{\circ}\text{C}$), high construction stability (survival rate of more than 80%), high storage stability (loss rate of 2.35% at 49 d), and high mechanical properties (Young's modulus and nano-hardness of 3.15 Gpa and 0.54 Gpa, respectively). Compared with microcapsules without nano-SiC, the thermal conductivity of the 10% nano-SiC-modified microcapsules increased by 21.6%, their specific heat capacity decreased by 10.45%, and their thermal diffusion coefficient increased by 36.96% after microwave heating for 6 min.

Keywords: microcapsules; nano-SiC; microstructure; chemical constitution; mechanical strength; stability



Citation: Sun, Y.; Ji, X.; Hou, Y.; Wang, S.; Chen, Y.; Liu, L.; Liu, S.

Characterization of Thermal and Stress Dual-Induced

Nano-SiC-Modified Microcapsules.

Coatings **2024**, *14*, 1573. <https://doi.org/10.3390/coatings14121573>

Academic Editor: Aivaras Kareiva

Received: 12 November 2024

Revised: 3 December 2024

Accepted: 10 December 2024

Published: 16 December 2024



Copyright: © 2024 by the authors. Licensee MDPI, Basel, Switzerland. This article is an open access article distributed under the terms and conditions of the Creative Commons Attribution (CC BY) license (<https://creativecommons.org/licenses/by/4.0/>).

1. Introduction

Cracks are a significant deterioration phenomenon affecting asphalt pavement and undergo a series of processes, including emergence, expansion, and penetration. Initially, microcracks emerge and then evolve into penetration joints under the combined influence of temperature and load cycles. The timely elimination of microcracks can inhibit or delay the formation of penetration joints [1].

Microcapsules represent a novel self-healing material for pavement microcracks [2,3]. Adsorption encapsulation and sharp pore coagulation bath methods are simpler and have low raw material costs but have a low content of vesicle cores ($\leq 40\%$) [4–7]. Moreover, the larger particle size of microcapsules (micron level) has a greater effect on the mechanical strength and stability of asphalt mixtures [8–10]. Microcapsules prepared by interfacial polymerization have a suitable particle size but are prone to agglomeration during the preparation process, and the shell thickness is difficult to precisely control [8–10]. Furthermore, the mechanical properties of microcapsules are poor (Young's modulus and hardness are 276.94 Mpa–408.90 Mpa and 43.38–71.08, respectively) [11,12]. In addition, microcapsules prepared by interfacial polymerization have poor thermal stability (the mass loss is

10%–15% at 160–180 °C) [12]. Compared with the previous three methods, microcapsules prepared by in situ polymerization have a higher capsule core content (64.08%–79.33%) and higher mechanical strength (Young's modulus (MPa) and hardness (MPa) are 1000–2700 and 37.66–140, respectively) [13–15]. Moreover, the shell thickness and core content can be adjusted during the preparation process. The microcapsules prepared by this method are thermally stable (the mass loss is 3.72%–20% at 140–180 °C), which ensures the survival of the microcapsules during the construction process [16]. Therefore, this method is the most widely used preparation method for application in the self-healing of pavements [17].

Conventional microcapsules are stress-triggered by the tip of a microcrack to release their core material. This passive and uncontrollable stress-induced mode does not ensure that the vesicle core material is released promptly and in an amount that matches the microcrack at the appropriate time [18,19]. Therefore, the development of stimulus-responsive controlled-release microcapsules is essential. Controlled-release microcapsules are particles with stimuli-responsive properties that are introduced into the capsule shell. In response to internal triggers (such as pH, temperature, or enzymes) or external stimuli (such as microwaves, light, ultrasound, and electric and magnetic fields), the capsule releases its encapsulated core material [18,20]. Nano-SiC exhibits excellent wave-absorbing and temperature-raising properties. Microcapsules prepared with a nano-SiC modifier doped into the capsule shell material can achieve a microwave-induced release of capsule core material and thermodynamic dual-induced release triggered by the stress at the tips of the microcracks. This represents a desirable and innovative approach for significantly enhancing the self-healing effect of microcracks in asphalt pavement [21,22].

Therefore, this study proposes a thermal and stress dual-induced nano-SiC microcapsule for asphalt pavement applications. Nano-SiC can endow microcapsules with good basic, stable, and mechanical properties to stabilize their presence in asphalt mixtures. In addition, nano-SiC-modified microcapsules have wave-absorbing and temperature-raising properties that enable them to achieve the dual-mechanism-induced release of rejuvenating agents.

2. Materials and Methods

2.1. Materials

Thermal dual-induced microcapsules are composed of modified capsule shell material and a regeneration agent. The modified capsule shell materials are composed of a highly methylated melamine formaldehyde resin (H3M) prepolymer and nano-SiC composite. The main components of the regeneration agent are aromatic and saturated phenols. In addition, a curing agent consisting of sodium chloride, resorcinol, and ammonium chloride is added to prepare the microcapsules. The modified microcapsules were prepared by in situ polymerization with the following main steps.

(1) The SDS emulsifier was added to deionized water at a mass ratio of 100/1.71 for mixing and stirring. The resulting mixture was then placed in a constant-temperature water bath at 30 °C for one hour. Then, a regenerator was added to achieve a mass ratio of emulsifier to regenerant of 1/4.97. The mixture was stirred at the shear rate of 3500 r/min to obtain a regenerated emulsion.

(2) H3M at a mass ratio of regenerant/H3M of 1.57/1 and nano-SiC at a ratio of SiC/H3M of 3/40 were added to the beaker. After stirring to achieve a uniform mixture, a small amount of deionized water was added to form a gray prepolymer solution. Then, the prepolymer solution was dispersed for 30 min by an ultrasonic disperser.

(3) The prepolymer solution of the composite capsule shell was dropped into the emulsion regenerant solution and mechanically stirred at a speed of 600 r/min at 30 °C for 30 min. In this process, sodium chloride, resorcinol, and ammonium chloride were gradually added, and the mass ratios to H3M were set at 0.99/1, 1/20.2, and 1/20.2, respectively.

(4) A 10% acetic acid solution was added dropwise to the mixed solution of the prepolymer and regenerator at a controlled rate of 2 mL/min. The pH of the solution

was adjusted to 4.5. The temperature of the mixed solution was then gradually increased to 70 °C at a rate of 2.5 °C/min, followed by stirring at 950 rpm for 3 h to obtain the microcapsule suspension.

(5) The resulting microcapsule suspension was vacuum filtered using a Brinell funnel and washed with deionized water and petroleum ether three times to remove the uncoated regenerate. Then, the cleaned microcapsules were filtered and placed in an oven at 60 °C for 1 h to obtain the yellow-brown microcapsules.

2.2. Testing Methods

2.2.1. Basic Properties

Particle Size Distribution

The particle size of the microcapsules was determined using fluorescence microscopy (FM, Phenix, Shangrao, China). First, the microcapsule samples were added to a test tube containing a small amount of anhydrous ethanol and dispersed using an ultrasonic disperser for 1 min until a homogeneous microcapsule–ethanol suspension was formed. Next, a small volume of the suspension was drawn onto a slide using a dropper and covered with a coverslip. The particle size was then observed and recorded using FM. Finally, the particle size distribution was quantified and statistically analyzed using Image-Pro Plus 6.0 (Media Cybernetics, Rockville Maryland, MD, USA), as shown in Figure 1.



Figure 1. Particle size distribution measurement method.

Microscopic Morphology and Capsule Shell Thickness

Scanning electron microscopy (SEM, Carl Zeiss AG, Oberkochen, Germany) was used to examine the microscopic morphology of the microcapsules and measure the thickness of the capsule shell. First, the microcapsule powder was dispersed in anhydrous ethanol and uniformly applied to the sample stage. The surface of the microcapsules was then cleaned by air-jetting with high-pressure gas. Finally, the microcapsules were observed, and the thickness of the capsule shell was quantified using SEM at magnification ranging from 200 to 60,000, as shown in Figure 2.

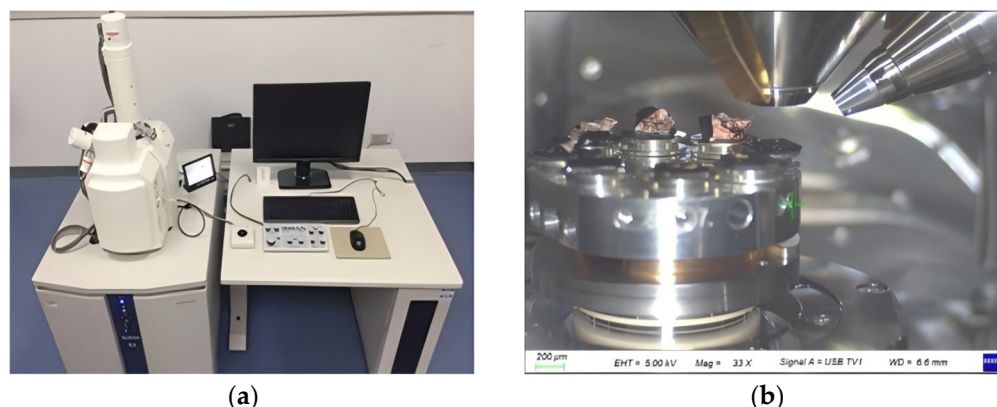


Figure 2. Scanning electron microscope and specimen. (a) scanning electron microscope and (b) specimen.

Chemical Structure

The chemical structure of the microcapsules was analyzed by Fourier transform infrared spectroscopy (FTIR, Thermo Nicolet, Waltham MA, USA). The FTIR spectra of the nano-SiC composite capsule shell, microcapsule, regenerant, and nano-SiC were obtained using the potassium bromide (KBr) pellet method. The solid samples were tested in the wave numbers of $4000\sim 400\text{ cm}^{-1}$, while the liquid samples were tested in the range of $4000\sim 600\text{ cm}^{-1}$. The changes in the characteristic peaks of each absorption spectrum were analyzed to determine whether the capsule shell fully encapsulated the core materials, thereby confirming the successful preparation of microcapsule.

Core Content

The content of the microcapsule core was determined by solvent extraction. First, the microcapsules at a certain mass (m_0) were weighed and crushed to destroy the capsule shell structure, allowing the regenerant to be completely released. The remaining microcapsules were then washed, cleaned, and dried to obtain the residue of the capsule shell, which represents the mass (m_s) of the composite capsule shell. The mass of the capsule core in the tested microcapsule sample is the difference between the microcapsule sample and the mass of the composite capsule shell. Therefore, the core content of the microcapsule (R_c) can be calculated by Equation (1) [23].

$$R_c = \frac{m_c}{m_0} \times 100\% = \frac{m_0 - m_s}{m_0} \times 100\% \quad (1)$$

2.2.2. Stability

Thermal Stability

A thermogravimetric analyzer was used to assess the thermal stability of the microcapsules. The thermal stability of the capsule shell material, core material, and microcapsules was tested in the temperature range of $30\sim 400\text{ }^\circ\text{C}$, with a heating rate of 10 K/min . High-purity nitrogen was used as the test gas, with a flow rate of 40 mL/min .

Storage Stability

The residual mass method was used to test the storage stability of the microcapsules. First, 420 g of dried microcapsules was equally divided into six sealed glass bottles, which were then placed in a cool, dry location and stored for a period protected from light. The residual mass of the microcapsules was measured at weeks 1, 2, 3, 4, 5, 6, and 7. The rate of mass loss was calculated using Equation (2) [24].

$$R_{mi} = \frac{m_0 - m_i}{m_0} \quad (2)$$

R_{mi} —Rate of mass loss of microcapsules at week i , %;
 m_0 —Mass of microcapsules before washing, g;
 m_i —Mass of microcapsules after washing, g;
 i —Number of weeks of storage, which were taken as 1, 2, 3, 4, 5, 6, and 7.

Construction Stability

The structural stability of microcapsules was tested by observation and statistics. First, an asphalt mixture containing 6% microcapsules was prepared. Once the mixture had cooled sufficiently, the asphalt and aggregate were separated using trichloroethylene (TCE) to produce the asphalt-containing microcapsules. Next, the morphology of the microcapsules in the extract was observed using FM. Finally, the survival rate of microcapsules was calculated. To quantitatively evaluate the survival rate of the microcapsules in the asphalt mixture, n_1 samples of the TCE extract from the microcapsule asphalt mixture were prepared, and n_2 monitoring points were randomly selected for FM observation. The total number of microcapsules was recorded as R_t , and the number of damaged microcapsules was recorded as R_l . The microcapsule survival rate was then calculated using Equation (3), and the microcapsule damage rates at all monitoring sites were averaged using Equation (4). The mean value from all observation points was then calculated to characterize the survival rate of microcapsules in the mixing process.

$$R = \left(1 - \frac{R_l}{R_t}\right) \times 100\% \quad (3)$$

$$\bar{R} = \frac{\sum_{i=1}^{n_1 \cdot n_2} R_i}{n_1 \cdot n_2} \quad (4)$$

\bar{R} —Overall survival of microcapsules, %;
 R_i —Survival of microcapsules at observation point i , %;
 n_1 —Number of samples of trichloroethylene extract;
 n_2 —Number of observation points.

2.2.3. Micromechanical Strength

The Young's modulus and nano-hardness of microcapsules were tested by a nanoindentation instrument. The load range of the nanoindentation is 0 ~ 500 mN, with a load accuracy is up to 0.05 nN and a displacement resolution of 0.01 nm. The procedure for preparing the microcapsule specimen for the nanoindentation test is as follows: ① cut the slides into squares; ② apply the pre-configured crystal adhesive to a square area of 1 cm × 1 cm and use a homogenizer to correct the thickness and flatness of the cemented layer; ③ spread the microcapsule samples on the surface of the unconsolidated crystal adhesive; ④ fix the samples for the loading stage of the nanoindentation test for subsequent experiments. The nano-hardness and Young's modulus of the microcapsules were calculated using the classic Oliver–Pharr analysis [25].

2.2.4. Thermodynamic Property

Microwave Heating Performance

The microwave heating performance of the microcapsules was tested using an infrared thermal imager and a microwave oven. First, 10 g of microcapsules was washed repeatedly with petroleum ether and then dispersed in anhydrous ethanol to remove any surface material that was not encapsulated by regenerated or unreacted H3M molecules. The cleaned microcapsules were then placed in an oven at 60 °C for 2 h to volatilize the residual water.

Next, the microcapsules were evenly distributed over an area of 1 cm² on the slide and covered with a coverslip to prevent them from scattering and ensure that each group received the same area of microwave radiation in the microwave oven. The slides were

then placed in a microwave heating cabinet for microwave heating. Finally, the infrared thermal images of the microcapsules were obtained using infrared thermography after the microwave heating, as shown in Figure 3.

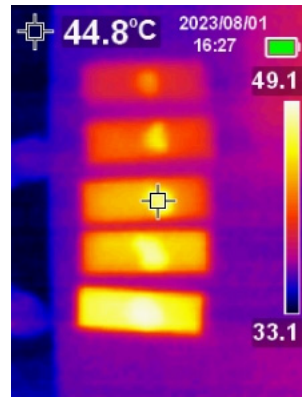


Figure 3. Infrared imaging of microcapsules.

Thermal Conductance

A thermal constant analyzer (Hot Disk, Gothenburg, Sweden) (shown in Figure 4) was used for thermal conductivity testing based on the Gustafsson transient plate heat source method [21] to accurately and rapidly evaluate the thermal conductivity of the microcapsules, including the heating coefficient, thermal conductivity, thermal diffusion coefficient, and specific heat capacity.



Figure 4. Thermal conductivity test sample and Hot Disk thermal constant analyzer: (a) thermal conductivity test samples; (b) Hot Disk thermal constant analyzer.

3. Results and Discussion

3.1. Basic Performance

3.1.1. Particle Size Distribution

The results of the particle size distribution of the microcapsules are shown in Figure 5. As seen in Figure 5a, the microcapsules exhibited good dispersibility, with no obvious agglomeration. From Figure 5b, it can be observed that the particle size of the microcapsules followed a normal distribution, with a maximum particle size of 98.79 μm and a minimum particle size of 12.37 μm . The particle size of most microcapsules (86.13%) ranges from 42 to 76 μm , with an average particle size of 53.5 μm .

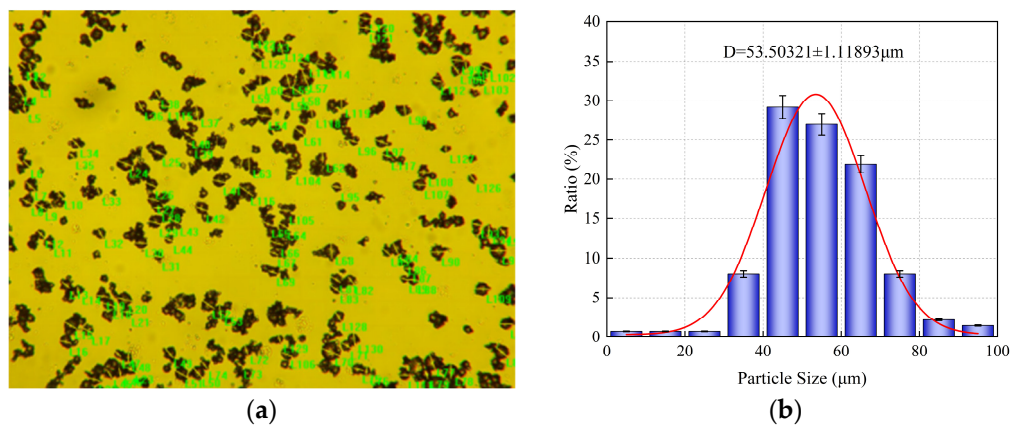


Figure 5. Particle size distribution test process and results: (a) particle size distribution test procedure; (b) particle size distribution test results.

Particle size has a significant influence on the properties and viability of microcapsules [26]. The particle size of microcapsules prepared by the adsorption encapsulation and sharp pore coagulation bath methods is in the millimeter range [27]. Excessive particle size exposes the microcapsules to damage during mixing and compaction, affecting the adhesion and mechanical strength of the asphalt to the aggregate. Microcapsules produced by the interfacial polymerization method have a small particle size (5–35 μm) and are prone to an electrostatic adsorption effect, resulting in obvious agglomeration [12]. Additionally, the thickness of the microcapsule shell is difficult to control, the core content is low, and the cost is high. Asphalt mastic film thickness is usually around 50 μm [13], and the particle size of the microcapsules prepared in this study is mainly concentrated in the range of 42–76 μm, so the microcapsules have little effect on the adhesion between the asphalt mastic and the aggregate. This also greatly reduces the likelihood of the aggregate experiencing mutual extrusion and early rupture during mixing and compaction, thus improving the survival rate of the microcapsules [28].

3.1.2. Microscopic Morphology and Shell Thickness

Figure 6 shows the SEM images of microcapsules under the optimal preparation process. It can be seen that both types of microcapsules are relatively regular in shape, though there are significant differences in their microscopic morphology. The surface of ordinary microcapsules is smooth and flat, with only a small number of resin blocks protruding. In contrast, the surface of the nano-SiC-modified microcapsules features a large number of rough and dense resin blocks, which increase the contact area between the microcapsules and the asphalt, thereby improving the adhesion performance between the two [29,30]. Additionally, the resin blocks contain nano-SiC particles, which enhance the strength of the microcapsules and improve their resistance to breakage during mixing and compaction. The shell of the microcapsules after rupture is shown in Figure 7. The thickness of the nano-SiC-modified microcapsule shell ranged from 1.5 μm to 2 μm, with an average thickness of 1.565 μm, accounting for only 3.9% of the average particle size of the microcapsule, and the shell thickness is relatively uniform.

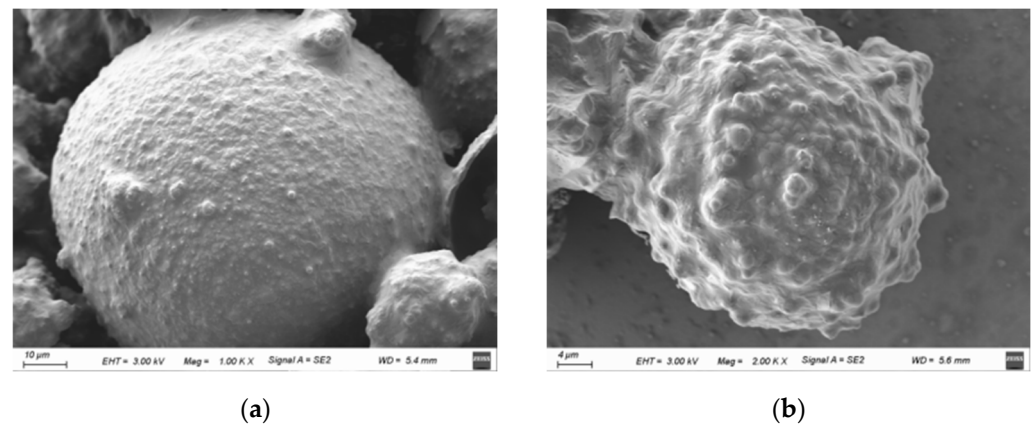


Figure 6. SEM morphology of microcapsules: (a) SEM morphology of undoped nanogram SiC-modified microcapsules; (b) SEM morphology of nano-SiC-modified microcapsules.

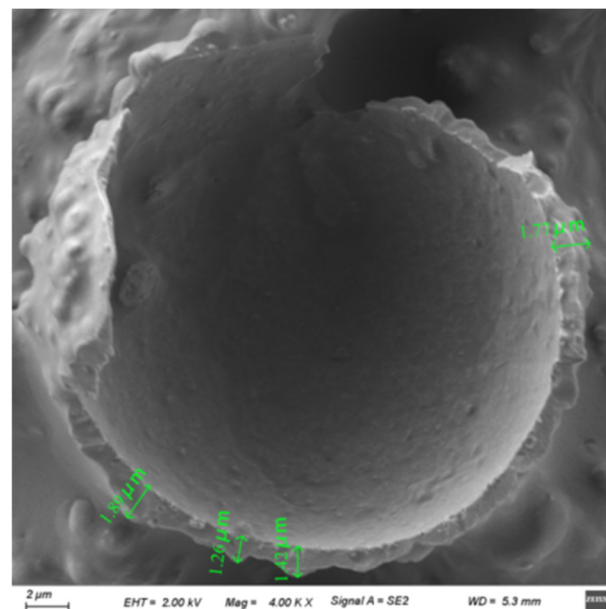


Figure 7. SEM image of microcapsule shell.

3.1.3. Chemical Structure

The changes in the characteristic peaks of each absorption curve in the infrared spectrum can be used to determine whether the microcapsules are successfully synthesized [31]. Figure 8 illustrates the infrared spectrograms of the nano-SiC-HMMM microcapsule shell, nano-SiC, microcapsules, and regenerant. The absorption peak at 843 cm^{-1} corresponds to the characteristic Si-C bond, and this peak is also observed in the microcapsule and microcapsule shell spectra. Furthermore, no new characteristic absorption peaks were detected in the microcapsules and microcapsule shell spectra, indicating that nano-SiC does not participate in the chemical reaction during the formation of the microcapsule shell. Instead, nano-SiC is likely adsorbed onto the surface of the H3M molecules through electrostatic interactions, thus remaining present in the microcapsules. Characteristic absorption peaks for the $-\text{CH}_3$ and $-\text{CH}_2$ stretching vibrations of the regenerant were observed at 1456 cm^{-1} and 2924 cm^{-1} , respectively [32].

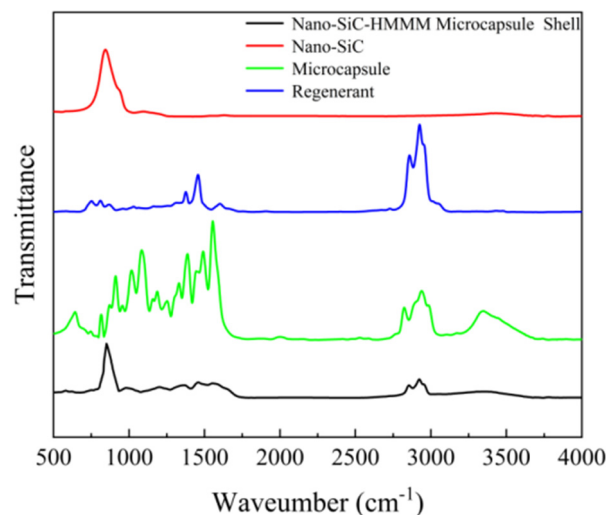


Figure 8. Infrared spectra of microcapsules.

The absorption peak at 1554 cm^{-1} corresponds to the characteristic bending deformation of the $-\text{N}=\text{C}=\text{N}-$ in melamine molecules, which is present in both microcapsules and microcapsule shell materials, confirming that the shell of microcapsules is formed by the dehydration and polymerization of H3M molecules under acidic conditions. As shown in Figure 8, the microcapsules exhibit all the characteristic peaks corresponding to the nano-SiC-HMMM microcapsule shell, nano-SiC, microcapsules, and regenerant, indicating that the thermal and stress dual-induced nano-SiC-modified microcapsules have been successfully prepared.

3.1.4. Core Content

The core contents of four groups of microcapsules were randomly detected, as shown in Table 1. The average core content of the dual-induced microcapsules was 87.6%, which increased the core content of the thermal dual-induced microcapsules by about 2–16 times compared to the existing calcium alginate microcapsules and porous sand microcapsules [6,7,33]. This is because calcium alginate microcapsules have multi-chamber structures, porous sand microcapsules have multi-core structures, and these complex shell structures significantly reduce the core content. However, thermal stress induced the inner shell of the microcapsules to become smooth, with the microcapsule shell containing only the regenerant. The core content of the double-induced microcapsules increased by 8.29%~23.54% compared to the in situ polymerization microcapsules and by 15.34%~17.22% compared to the interfacial polymerization microcapsules [5,14,34]. This is because the microcapsule shell prepared in this paper is 2~3 μm thick, which provides more space for storing the regenerant. The reason is due to the combination of modified materials and resin molecules, which improves the mechanical properties of the microcapsule shell materials, thereby increasing the core content. A higher core content indicates better self-healing performance [27,35,36].

Table 1. The core content of microcapsules.

Specimens	1	2	3	4	Average
Core content /%	84.01	89.76	88.52	88.19	87.62

3.2. Stability

3.2.1. Thermal Stability

Figure 9 shows the TGA curves of the microcapsules, shell material, and core material. As the temperature increases, the mass loss of microcapsules gradually increases. The mass loss process can be divided into three main stages. The first stage occurs between

30 and 200 °C, where the mass loss of the microcapsule is small, accounting for only 5.642% of the total microcapsule. During this stage, the mass loss is primarily due to the evaporation of water within the microcapsules, as well as the degradation of small molecules from the polymer that are not fully cross-linked or cured [37]. The second stage occurs between 200 and 420 °C, where the mass of the microcapsules decreases rapidly. The DTG curves of the shell material show that the surface layer of the shell undergoes violent decomposition, leading to a gradual thinning of the capsule shell, and eventually, the microcapsules rupture. At this point, the core material is directly exposed to the high-temperature environment, experiencing extremely rapid thermal decomposition, which significantly damages the quality of the microcapsules [38]. From the curve in this stage, it can be seen that the thermal stability of the microcapsules is significantly higher than that of the shell material, indicating that the addition of nano-SiC effectively improves the thermal stability of the microcapsules. In the third stage (>700 °C), the residual mass of the microcapsules is significantly higher than that of both the shell and core material. This is due to the excellent thermal stability of nano-SiC, which hardly decomposes at 700 °C. Compared with the existing microcapsules, the thermal stress dual-induced nano-SiC microcapsules prepared in this study exhibit better thermal stability, with a mass loss rate of only 2.919% in the temperature range used for construction mixing (150–170 °C), which is much smaller than that of interfacial polymerization microcapsules, calcium alginate microcapsules, and porous sand microcapsules. Meanwhile, the addition of suitable modifiers of the capsule shell materials (such as nano-SiC, nano-SiO₂ carbide, etc.) can significantly improve the high-temperature resistance of microcapsules [2]. This is because the addition of inorganic modified materials makes the shell of the microcapsules denser and improves their resistance to high-temperature deformation, while the rough shell surface also provides more space for high-temperature deformation. Compared with other microcapsules, the mass loss of the nano-SiC-modified microcapsules is reduced by 5%~15% at the same temperature [24].

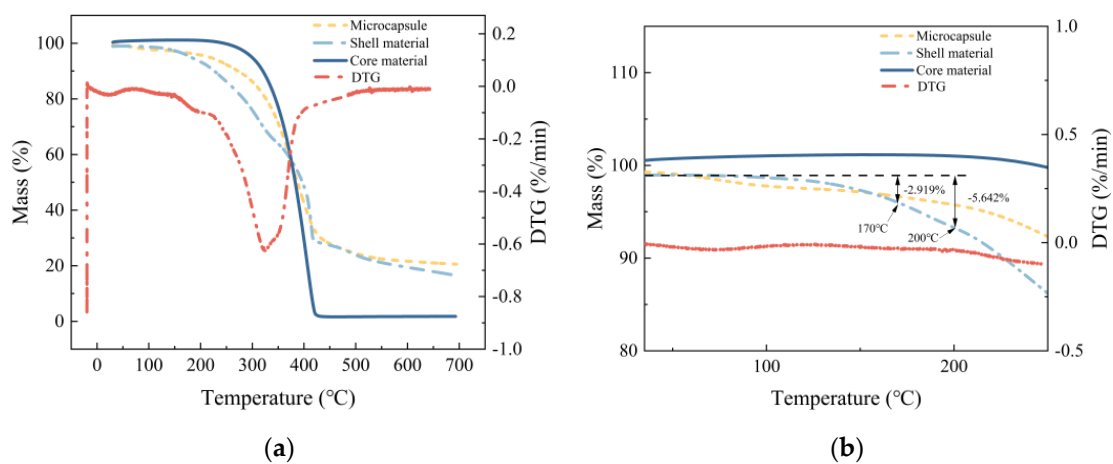


Figure 9. Mass loss of microcapsules. (a) is mass loss of microcapsules at room temperature to 700 °C; (b) is enlarged view of mass loss of microcapsules at room temperature to 300 °C.

3.2.2. Storage Stability

Figure 10 demonstrates the variation in the mass loss of microcapsules over different storage periods (7 d, 14 d, 21 d, 28 d, 35 d, 42 d, and 49 d). The fastest mass loss of microcapsules was observed during the first 7 days, due to the small amount of uncondensed H₃M molecules and water on the surface of the microcapsules, which volatilized rapidly into the air [39]. The mass loss of the microcapsules gradually increased with the extension of the storage time. This may be due to the prolonged storage resulting in exposure of the shell material to air oxidation [24]. In addition, the regenerant may also be exposed to air infiltration through weak portions of the shell and slowly volatilize, further contributing to

the mass loss of the microcapsules. As the storage time continued to increase, the mass loss rate of the microcapsules decreased and gradually stabilized (with a 2.25% mass loss after 49 d), indicating that the microcapsules have good storage stability [40].

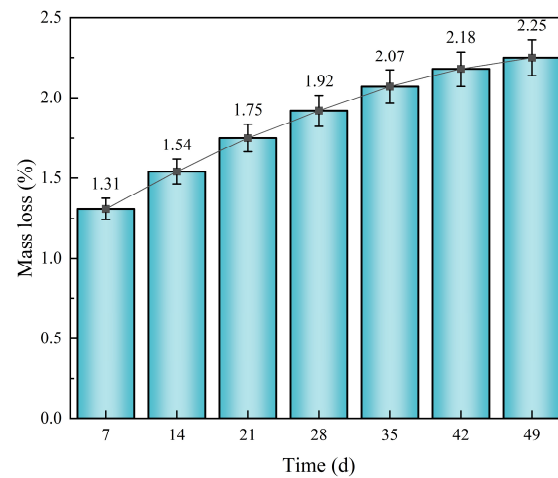


Figure 10. Rate of mass loss of microcapsules at different storage days.

3.2.3. Construction Stability

To investigate the construction stability of the microcapsules, FM was used to observe their morphology in asphalt mixture extracts. Asphalt mixtures were prepared at 130 °C and 160 °C with 6% microcapsules. The results are shown in Figure 11. It was found that most of the microcapsules maintained an intact structure with no leakage of the core material after mixing and compression at 130 °C and 160 °C. In addition, a few microcapsules retained their intact circular morphology, although the internal core material was prone to leakage, causing the fluorescence of the microcapsules to be significantly reduced under FM.

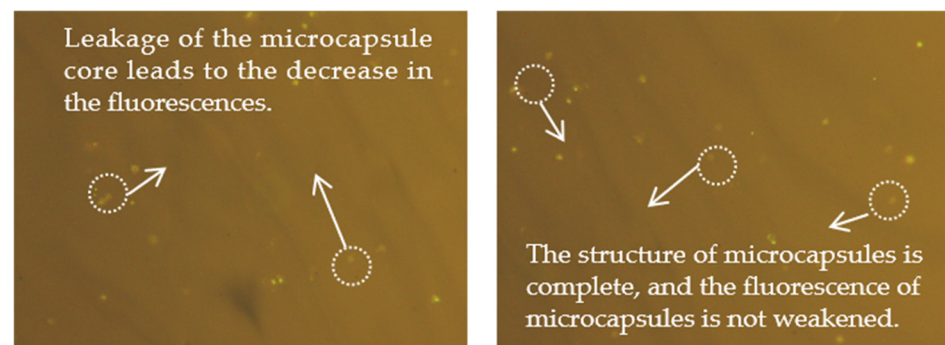


Figure 11. Fluorescence microscopy images of surviving microcapsules in asphalt mixes.

Based on the survival state of microcapsules observed under FM, mathematical and statistical methods were used to roughly estimate their survival rate after construction mixing [41]. The results are shown in Figure 12. The microcapsules remained highly viable under high-temperature mixing, with survival rates of 82.66% at 130 °C and 79.12% at 160 °C. As the temperature increased, the survival rate of microcapsules produced a certain decrease. This was because the higher temperature softened the resin components in the microcapsule shell, reducing its strength, while the thermal expansion of the core material caused the microcapsule shell to expand, further increasing the likelihood of damage to the microcapsule shell. During the statistical process, it was found that microcapsules with a particle size larger than 60 μm were more likely to rupture. This is because microcapsules with larger particle sizes cannot be protected by the asphalt film on the aggregate surface and are more likely to be crushed directly by the aggregate [27].

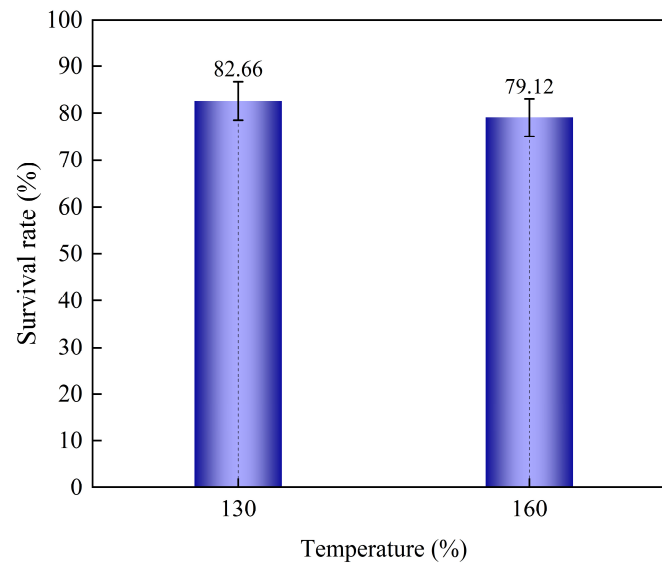


Figure 12. Survival of microcapsules at 130 °C and 160 °C mixing temperatures.

3.3. Mechanical Strength

Figure 13 shows the nanoindentation force–displacement curves of the modified microcapsules with different nano-SiC contents. The testing results of Young’s modulus and nano-hardness are shown in Table 2. The mechanical strength of the microcapsules increased gradually with the increase in nano-SiC content. When the nano-SiC content increased from 0% to 10%, the nano-hardness increased from 0.26 Gpa to 0.54 Gpa, and the Young’s modulus increased from 2.45 Gpa to 3.15 Gpa. This is because the nano-SiC combines with resin molecules to form a three-dimensional structure with alternating rigid parts (nano-SiC) and flexible parts (H3M), which improves the mechanical strength of the shell material. This ensures the survival of the microcapsules during the construction of asphalt mixtures. Compared with the existing microcapsules, the Young’s modulus and nano-hardness of the dual-induced nano-SiC-modified microcapsules prepared in this paper were increased by about 20%–290% and 63.6%–760%, respectively. This indicates that the hardness and content of the modified materials have an important effect on the mechanical strength of the microcapsule shell, proving that the modification of the microcapsule shell with high-strength nanomaterials is an effective way to improve the mechanical strength of the microcapsules. Compared with other microcapsules, the Young’s modulus and nano-hardness of the nano-SiC-modified microcapsules increased by 1.5 times and 3.0 times, respectively [6,7,12,14–16].

Table 2. Results of Young’s modulus and nano-hardness test of microcapsules.

Mechanical Parameter	Nano-SiC Doping (%)				
	0	2.5	5	7.5	10
Nano-hardness (Gpa)	0.26	0.31	0.39	0.50	0.54
Young’s modulus (Gpa)	2.45	2.62	2.91	3.07	3.15

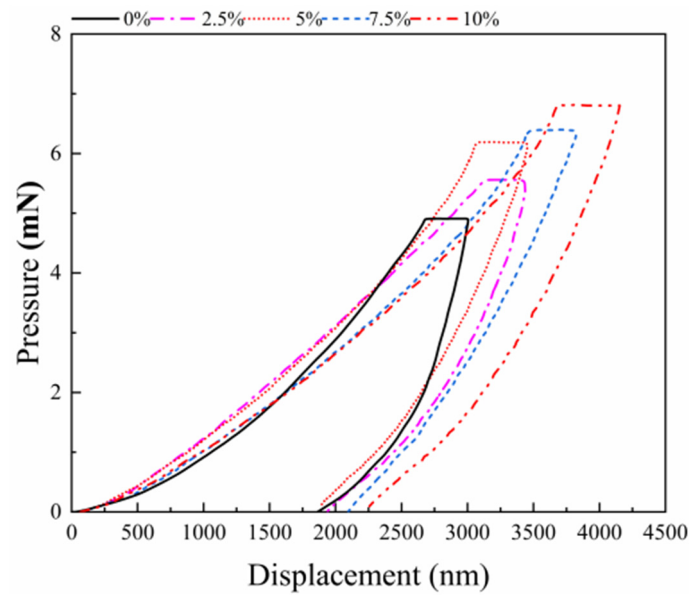


Figure 13. Nanoindentation force–displacement curve.

3.4. Thermodynamic Property

3.4.1. Microwave Heating Performance

To investigate the effect of nano-SiC content on the microwave heating performance of microcapsules, infrared thermography was used to monitor the temperature changes of microcapsules with different nano-SiC contents (0%, 2.5%, 5%, 7.5%, and 10%) in real time at different heating times (1.5 min, 3 min, 4.5 min, and 6 min). The results are shown in Table 3.

Table 3. Results of microwave heating characteristics of different kinds of microcapsules (°C).

Nano-SiC Doping (%)	Microwave Heating Time (min)			
	1.5	3.0	4.5	6.0
0	36.2	37.1	38.7	39.4
2.5	38.1	40.7	45.6	48.6
5.0	44	44.8	48.2	54.7
7.5	45.5	47.9	50.9	57.0
10	46.1	49.1	52.5	58.6

The microwave heating effect of the microcapsules gradually increased with the increase in nano-SiC content. The temperature of the microcapsules with 10% nano-SiC was 48.73% higher than that of the microcapsules without nano-SiC after the same heating time (6 min). When the nano-SiC content was 0%, the temperature difference between the microcapsules after heating for 1.5 min and 6 min was only 3.2 °C. This is due to heat accumulation caused by prolonged heating. When the nano-SiC content was 10%, the temperature of the microcapsules reached 58.6 °C after 6 min of heating, and the heating effect was significant. It was enhanced by 48.73% compared to heating for 1.5 min. However, for the same heating time (6 min), the temperature of the microcapsules with 7.5% nano-SiC increased by only 4.2% compared with that of the microcapsules with 5% nano-SiC, indicating that the enhancement of the microwave heating characteristics of the microcapsules was gradually weakened by a nano-SiC content higher than 5%. In addition, the heating rate of the microcapsules increased with the prolongation of microwave heating time. When the microwave heating time was 3 min, the warming rate was 2 °C/min, and when the microwave heating time was 6 min, the warming rate was 4.07 °C/min. This is because the coupling of nanosized SiC with microwave radiation

has a more significant warming effect on enhancing absorption after arriving at a certain temperature [42]. Combining the economic factors, the extended microwave heating time required to increase the temperature of the microcapsules is preferred.

3.4.2. Thermal Conductivity

To investigate the effect of different nano-SiC contents on the thermal conductivity of microcapsules, microcapsules with different nano-SiC contents (0%, 2.5%, 5%, 7.5%, and 10%) were tested using a hot plate thermal constant meter. The results are shown in Figure 14.

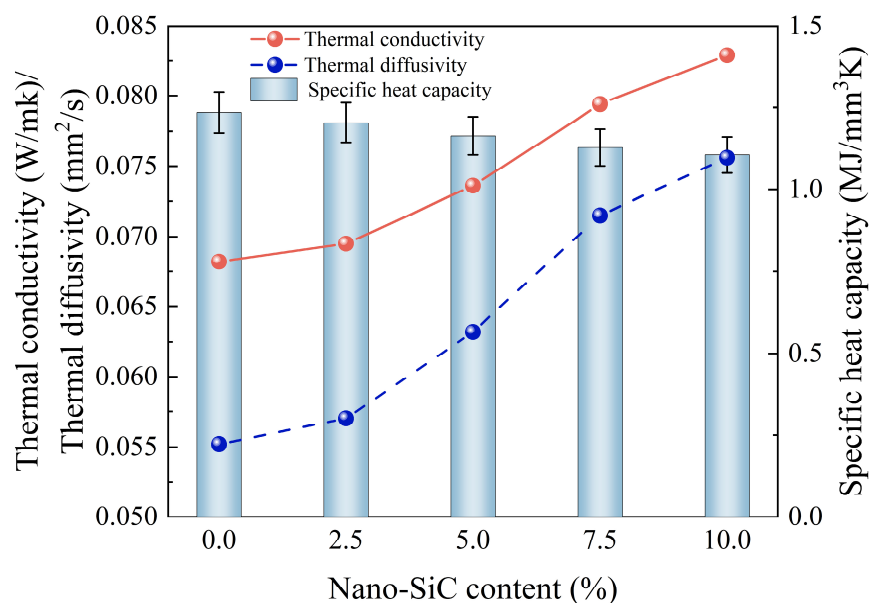


Figure 14. Thermal conductivity of microcapsules with different contents of nano-SiC.

The thermal conductivity of the microcapsules increased gradually with the increase in nano-SiC content. When the nano-SiC content was 10%, the thermal conductivity of the microcapsules increased by 21.6% compared to that of the microcapsules without nano-SiC. In addition, the specific heat capacity of the microcapsules decreased significantly, indicating that the microcapsules warmed up faster after thermal radiation. The accelerated warming rate of the microcapsules would reduce the time required for the core material to fill the microcracks, thus improving the self-healing efficiency of microcapsules. It can be observed that the thermal diffusion coefficient of the microcapsules gradually increases with the increase in nano-SiC content. This property helps transfer heat, which contributes to the rapid warming of the asphalt material around the microcapsules, and thus positively promotes the diffusion and penetration of the repair agent as well as the diffusion of asphalt molecules [43].

3.5. Self-Healing Mechanism

To investigate the self-healing behavior of the stress dual-induced nano-SiC-modified microcapsules, fluorescence microscopy was used to observe the state of microcracks in asphalt with a 6% microcapsule content. Under the fluorescence microscope, the asphalt and regenerant agents emit deep orange and yellow-green fluorescence, respectively, allowing observation of the distribution of the regenerant agents around the cracks.

As seen from Figure 15, a certain amount of the microcapsules in the asphalt show yellow fluorescence. As the microcrack passes over the location of the microcapsule, the microcapsule is punctured and releases a yellow-green regenerant. It can be observed that the microcapsules darkened, and the fluorescence significantly decreased. The regenerant flowed and diffused around the microcracks by capillary action. Under the action of

microwave heating, the temperature of the microcapsules gradually increased, and this flow–diffusion phenomenon was accelerated, further promoting the healing of microcracks. At this time, both sides of the microcrack emitted yellow-green fluorescence, and the width of the microcrack was reduced, indicating that the regenerant had successfully repaired the microcrack.

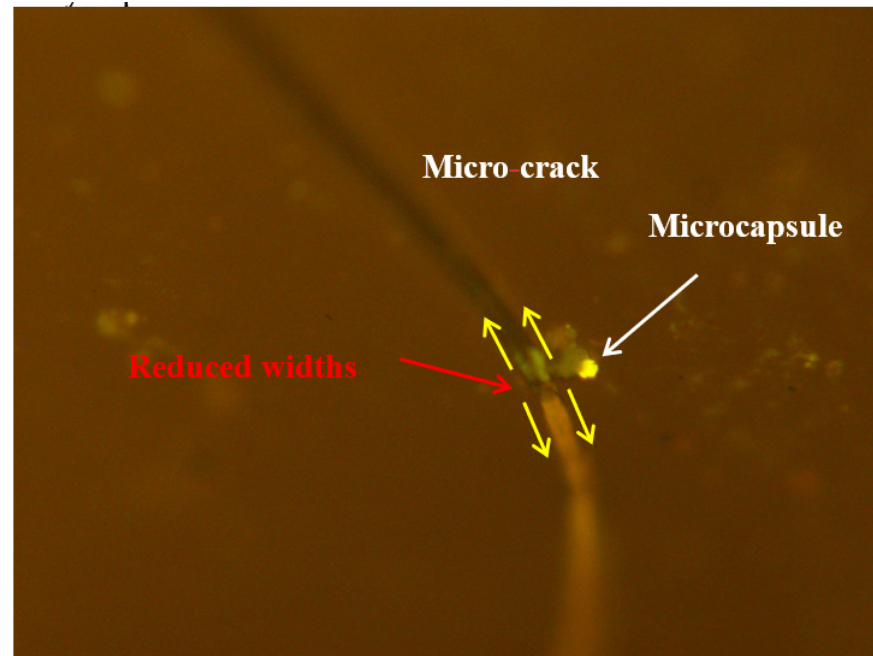


Figure 15. Self-healing process of microcapsule.

3.6. Comparison of the Prepared Nano-SiC-Modified Microcapsules with Other Microcapsules

The results of the comparative analysis of the technical performance of the nano-SiC-modified microcapsules and other microcapsules are shown in Table 4. The results show that the average particle size of the nano-SiC-modified microcapsules was 53.50 μm , and the core content reached 87.6%, which was an increase of 2~23% compared to other road microcapsules. Meanwhile, through process optimization and improvement, the mass loss of microcapsules in the temperature range of 150–170 $^{\circ}\text{C}$ was only 2.92%, which was 5%~15% lower than that of other microcapsules. The Young's modulus and nano-hardness of the 10% SiC-modified microcapsules reached 3.15 Gpa and 0.54 Gpa, respectively. Compared to other microcapsules, the Young's modulus and nano-hardness of the nano-SiC-modified microcapsules are increased by 1.5 times and 3.0 times, respectively [6,7,12,14–16]. After microwave heating for 6 min, the thermal conductivity of the 10% nano-SiC-modified microcapsules increased by 21.6%, the specific heat capacity decreased by 10.45%, and the heat diffusion coefficient increased by 36.96%, compared to that of microcapsules without nano-SiC.

Table 4. Comparison of the prepared nano-SiC-modified microcapsules with other microcapsules.

Microcapsule Type	Particle Size/ μm	Core Content/%	Mechanical Strength	Thermal Stability (Temperature $^{\circ}\text{C}$ /Mass Loss Ratio %)
Adsorption encapsulation [6]	1–10 mm	20	Ultimate resistance (N)/deformation (μm) 17.61/106.92	180/3
Piercing solidification method [7,33]	1–6.8 mm	40	Uniaxial compression 130 $^{\circ}\text{C}$ /12N Young's Modulus (MPa)/ hardness (MPa) 276.94–408.90 43.38–71.08	200/4
Interfacial polymerization [12,34]	5–35	70.40–72.28	Young's Modulus (MPa)/ hardness (MPa) 1000–2700 37.66–140	160–180/10–15
In situ polymerization [14–16,35]	2–230	64.08–79.33	Young's Modulus (MPa)/ hardness (MPa) 2620–3150 310–540	140–180/3.72–20
Nano-SiC-modified microcapsules	40–100	87.62		140–200/4.257

4. Conclusions

The study of thermal and stress dual-induced nano-SiC microcapsules is highly significant to the field of microcapsule self-repair. In this paper, the core content, stability, and mechanical properties of the microcapsules were significantly improved by doping nano-SiC into the microcapsule shell. In addition, doping nano-SiC simultaneously significantly improved both the microwave warming performance and thermal conductivity of the microcapsules. Compared to other microcapsules, the core content of these microcapsules was increased by 8.29–23.54%, the thermal mass loss was reduced by 5%–15% at the same temperature, and the mechanical strength was enhanced by 1.5 times and 3.0 times. Additionally, compared to microcapsules without nano-SiC, the thermal conductivity and microwave heating performance of the microcapsules with 10% nano-SiC increased by 21.6% and 48.73%, respectively, enabling the thermal induction and core release in the modified microcapsules. Further research is needed to explore the trade-offs between the performance and benefits of microcapsules in practical engineering. Despite these challenges, this study provides valuable insights into the in-depth exploration of microcapsules in the field of asphalt self-repair and suggests directions for the study of novel microcapsules. The authors anticipate future research that builds upon, scrutinizes, and refines the findings of this study, further contributing to this critical area of study.

Author Contributions: Investigation, Y.S. and Y.C.; writing—original draft, S.W. and Y.C.; funding acquisition, Y.S., X.J. and Y.H.; supervision, X.J. and Y.H.; formal analysis, S.W. and Y.C.; writing—review and editing, L.L. and S.L. All authors have read and agreed to the published version of the manuscript.

Funding: This research was funded by the Natural Science Foundation of Xinjiang Uygur Autonomous Region under Grant No. 2023D01A88, the Natural Science Basic Research Program of Shaanxi Province under Grant No. 2024JC-YBMS-435, and the Fundamental Research Funds for the Central Universities of CHD under Grant No. 300102214909.

Institutional Review Board Statement: Not applicable.

Informed Consent Statement: Not applicable.

Data Availability Statement: The data presented in this study are available upon request from the corresponding author.

Conflicts of Interest: Author Yunlong Sun and Sijia Liu was employed by the company Xinjiang Academy of Transportation Science, Co., Ltd. The remaining authors declare that the research was conducted in the absence of any commercial or financial relationships that could be construed as a potential conflict of interest.

References

1. Ji, X.; Yang, Z.; Zhou, Z.; Zhang, Y.; Lei, Y. Evaluation method for self-healing performance of densely graded asphalt mixture. *J. Chin. Highw.* **2018**, *31*, 51–57. (In Chinese) [[CrossRef](#)]
2. Lu, T.; Li, B.; Sun, D.; Hu, M.; Ma, J.; Sun, G. Advances in controlled release of microcapsules and promising applications in self-healing of asphalt materials. *J. Clean. Prod.* **2021**, *294*. [[CrossRef](#)]
3. He, L.; Huang, H.; Wim, V.; Tóth, C.; Gao, J.; Kowalski, K.; Jan, V. A state-of-the-art on microcapsules for asphalt self-healing. *Cailiao Daobao* **2020**, *34*, 15092–15101. (In Chinese) [[CrossRef](#)]
4. He, L.; Zhao, L.; Ling, T. Research on the induced thermal self-healing performance of cracks in dense asphalt mixtures. *J. Chin. Highw.* **2017**, *30*, 17–24. (In Chinese)
5. García, Á.; Schlangen, E.; van de Ven, M.; Sierra-Beltrán, G. Preparation of capsules containing rejuvenators for their use in asphalt concrete. *J. Hazard. Mater.* **2010**, *184*, 603–611. [[CrossRef](#)]
6. Liu, L.; Wu, F.; Ju, X.; Xie, R.; Wang, W.; Niu, C.; Chu, L. Preparation of monodisperse calcium alginate microcapsules via internal gelation in microfluidic-generated double emulsions. *J. Colloid Interface Sci.* **2013**, *404*, 85–90. [[CrossRef](#)]
7. Micaelo, R.; Al-Mansoori, T.; Garcia, A. Study of the mechanical properties and self-healing ability of asphalt mixture containing calcium-alginate capsules. *Constr. Build. Mater.* **2016**, *123*, 734–744. [[CrossRef](#)]
8. Garcia, A.; Jelfs, J.; Austin, C.J. Internal asphalt mixture rejuvenation using capsules. *Constr. Build. Mater.* **2015**, *101*, 309–316. [[CrossRef](#)]
9. Xu, S.; Tabaković, A.; Liu, X.; Palin, D.; Schlangen, E. Optimization of the calcium alginate capsules for self-healing asphalt. *Appl. Sci.* **2019**, *9*, 468. [[CrossRef](#)]
10. Zhang, L.; Liu, Q.; Li, H.; Norambuena-Contreras, J.; Wu, S.; Bao, S.; Shu, B. Synthesis and characterization of multi-cavity Ca-alginate capsules used for self-healing in asphalt mixtures. *Constr. Build. Mater.* **2019**, *211*, 298–307. [[CrossRef](#)]
11. Liu, X.; Zhang, H.; Wang, J.; Wang, Z.; Wang, S. Preparation of epoxy microcapsule based self-healing coatings and their behavior. *Surf. Coat. Technol.* **2012**, *206*, 4976–4980. [[CrossRef](#)]
12. Ji, X.; Li, J.; Hua, W.; Hu, Y.; Si, B.; Chen, B. Preparation and performance of microcapsules for asphalt pavements using interfacial polymerization. *Constr. Build. Mater.* **2021**, *289*, 123179. [[CrossRef](#)]
13. Li, J.; Ji, X.; Tang, Z.; Hu, Y.; Hua, W. Preparation and evaluation of self-healing microcapsules for asphalt based on response surface optimization. *J. Appl. Polym. Sci.* **2021**, *139*. [[CrossRef](#)]
14. Zhang, H.; Bai, Y.; Cheng, F. Rheological and self-healing properties of asphalt binder containing microcapsules. *Constr. Build. Mater.* **2018**, *187*, 138–148. [[CrossRef](#)]
15. Sun, D.; Hu, J.; Zhu, X. Size optimization and self-healing evaluation of microcapsules in asphalt binder. *Colloid Polym. Sci.* **2015**, *293*, 3505–3516. [[CrossRef](#)]
16. Wang, Y.-Y.; Tan, Y.-Q. Preparation, with graphene, of novel biomimetic self-healing microcapsules with high thermal stability and conductivity. *Front. Struct. Civ. Eng.* **2023**, *17*, 1–11. [[CrossRef](#)]
17. Su, J.-F.; Schlangen, E.; Qiu, J. Design and construction of microcapsules containing rejuvenator for asphalt. *Powder Technol.* **2013**, *235*, 563–571. [[CrossRef](#)]
18. Bao, C.; Xu, Y.; Zheng, C.; Nie, L.; Yang, X. Rejuvenation effect evaluation and mechanism analysis of rejuvenators on aged asphalt using molecular simulation. *Mater. Struct.* **2022**, *55*, 1–16. [[CrossRef](#)]
19. Wan, P.; Liu, Q.; Wu, S.; Zhao, Z.; Chen, S.; Zou, Y.; Rao, W.; Yu, X. A novel microwave induced oil release pattern of calcium alginate/ nano-Fe₃O₄ composite capsules for asphalt self-healing. *J. Clean. Prod.* **2021**, *297*, 126721. [[CrossRef](#)]
20. Wang, X.; Guo, Y.; Su, J.; Zhang, X.; Wang, Y.; Tan, Y. Fabrication and Characterization of Novel Electrothermal Self-Healing Microcapsules with Graphene/Polymer Hybrid Shells for Bitumenious Material. *Nanomaterials* **2018**, *8*, 419. [[CrossRef](#)]
21. Wang, Y.-Y.; Su, J.-F.; Schlangen, E.; Han, N.-X.; Han, S.; Li, W. Fabrication and characterization of self-healing microcapsules containing bituminous rejuvenator by a nano-inorganic/organic hybrid method. *Constr. Build. Mater.* **2016**, *121*, 471–482. [[CrossRef](#)]
22. Liang, Y.; Wang, T.; He, Z.; Sun, Y.; Song, S.; Cui, X.; Cao, Y. High thermal storage capacity phase change microcapsules for heat transfer enhancement through hydroxylated-silanized nano-silicon carbide. *Energy* **2023**, *285*, 129502. [[CrossRef](#)]
23. Li, B.; Sun, G.; Sun, D.; Lu, T.; Ma, J.; Deng, Y. Survival and activation behavior of microcapsules in self-healing asphalt mixture. *Constr. Build. Mater.* **2020**, *260*, 119719. [[CrossRef](#)]
24. Ji, X.; Wang, S.; Yao, B.; Si, W.; Wang, C.; Wu, T.; Zhang, X. Preparation and properties of nano-SiO₂ modified microcapsules for asphalt pavement. *Mater. Des.* **2023**, *229*, 111871. [[CrossRef](#)]

25. Oliver, W.; Pharr, G. An improved technique for determining hardness and elastic modulus using load and displacement sensing indentation experiments. *J. Mater. Res.* **1992**, *7*, 1564–1583. [[CrossRef](#)]
26. Norambuena-Contreras, J.; Concha, J.; Valdes-Vidal, G.; Wood, C. Optimised biopolymer-based capsules for enhancing the mechanical and self-healing proper-ties of asphalt mixtures. *Mater. Struct.* **2024**, *57*, 236. [[CrossRef](#)]
27. Al-Mansoori, T.; Micaelo, R.; Artamendi, I.; Norambuena-Contreras, J.; Garcia, A. Microcapsules for self-healing of asphalt mixture without compromising mechanical performance. *Constr. Build. Mater.* **2017**, *155*, 1091–1100. [[CrossRef](#)]
28. Liang, B.; Lan, F.; Shi, K.; Qian, G.; Liu, Z.; Zheng, J. Review on the self-healing of asphalt materials: Mechanism, affecting factors, assessments and improvements. *Constr. Build. Mater.* **2020**, *266*, 120453. [[CrossRef](#)]
29. He, L.; Cai, Z.; Feng, C.; Garcia, A.; Ma, Y. Review of research on microcapsule self-healing technology of asphalt mixtures. *J. Chang. Univ. (Nat. Sci. Ed.)* **2018**, *38*, 9–18, 77. [[CrossRef](#)]
30. Zhang, H.; Yao, T.; Li, C. Study on the mechanical behavior of microcapsules during the mixing process of asphalt mixture. *Constr. Build. Mater.* **2024**, *441*, 137531. [[CrossRef](#)]
31. Sun, D.; Pang, Q.; Zhu, X.; Tian, Y.; Lu, T.; Yang, Y. Enhanced Self-Healing Process of Sustainable Asphalt Materials Containing Microcapsules. *ACS Sustain. Chem. Eng.* **2017**, *5*, 9881–9893. [[CrossRef](#)]
32. Sun, D.; Sun, G.; Zhu, X.; Guarin, A.; Li, B.; Dai, Z.; Ling, J. A comprehensive review on self-healing of asphalt materials: Mechanism, model, characterization and enhancement. *Adv. Colloid Interface Sci.* **2018**, *256*, 65–93. [[CrossRef](#)] [[PubMed](#)]
33. Norambuena-Contreras, J.; Liu, Q.; Zhang, L.; Wu, S.; Yalcin, E.; Garcia, A. Influence of encapsulated sunflower oil on the mechanical and self-healing properties of dense-graded asphalt mixtures. *Mater. Struct.* **2019**, *52*, 1–13. [[CrossRef](#)]
34. Chung, K.; Lee, S.; Park, M.; Yoo, P.; Hong, Y. Preparation and characterization of microcapsule-containing self-healing asphalt. *J. Ind. Eng. Chem.* **2015**, *29*, 330–337. [[CrossRef](#)]
35. Tan, X.; Zhang, J.; Guo, D.; Sun, G.; Zhou, Y.; Zhang, W. Preparation and Repeated Repairability Evaluation of Sunflower Oil-Type Microencapsulated Filling Materials. *J. Nanosci. Nanotechnol.* **2020**, *20*, 1554–1566. [[CrossRef](#)]
36. Su, J.-F.; Wang, L.-Q.; Xie, X.-M.; Gao, X. Understanding the final surface state of self-healing microcapsules containing rejuvenator in bituminous binder of asphalt. *Colloids Surfaces A Physicochem. Eng. Asp.* **2021**, *615*. [[CrossRef](#)]
37. Zhang, H.; Wang, R.; Cheng, F. Study on the properties and self-healing ability of asphalt and asphalt mixture containing methanol-modified melamine-formaldehyde microcapsules. *Mater. Today Commun.* **2024**, *41*. [[CrossRef](#)]
38. Khorasani, S.N.; Ataei, S.; Neisiany, R.E. Microencapsulation of a coconut oil-based alkyd resin into poly(melamine-urea-formaldehyde) as shell for self-healing purposes. *Prog. Org. Coatings* **2017**, *111*, 99–106. [[CrossRef](#)]
39. Yang, P.; Han, S.; Su, J.; Wang, Y.; Zhang, X.; Han, N.; Li, W. Design of self-healing microcapsules containing bituminous rejuvenator with nano-CaCO₃/organic composite shell: Mechanical properties, thermal stability, and compactability. *Polym. Compos.* **2017**, *39*, E1441–E1451. [[CrossRef](#)]
40. Shirzad, S.; Hassan, M.; Aguirre, M.; Mohammad, L.; Cooper, S.; Negulescu, I. Microencapsulated Sunflower Oil for Rejuvenation and Healing of Asphalt Mixtures. *J. Mater. Civ. Eng.* **2017**, *29*, 04017147. [[CrossRef](#)]
41. Ji, X.; Yao, Z.; Si, W.; Wang, C.; Yi, K.; He, S.; Zhang, X. Self-healing behavior and microscopic mechanism of microencapsulated asphalt. *J. Traffic Transp. Eng. Engl. Ed.* **2023**, *23*, 67–77. [[CrossRef](#)]
42. Wang, X.; Li, C.; Zhao, T. Fabrication and characterization of poly(melamine-formaldehyde)/silicon carbide hybrid microencapsulated phase change materials with enhanced thermal conductivity and light-heat performance. *Sol. Energy Mater. Sol. Cells* **2018**, *183*, 82–91. [[CrossRef](#)]
43. Zhang, B.; Li, S.; Fei, X.; Zhao, H.; Lou, X. Enhanced mechanical properties and thermal conductivity of paraffin microcapsules shelled by hydrophobic-silicon carbide modified melamine-formaldehyde resin. *Colloids Surf. A Physicochem. Eng. Asp.* **2020**, *603*, 125219. [[CrossRef](#)]

Disclaimer/Publisher’s Note: The statements, opinions and data contained in all publications are solely those of the individual author(s) and contributor(s) and not of MDPI and/or the editor(s). MDPI and/or the editor(s) disclaim responsibility for any injury to people or property resulting from any ideas, methods, instructions or products referred to in the content.